IEEE Access
Multidisciplinary : Rapid Review : Open Access Journal

Received December 2, 2017, accepted January 15, 2018, date of publication January 23, 2018, date of current version March 9, 2018.

Digital Object Identifier 10.1109/ACCESS.2018.2797003

Frequency and Time-Frequency Analysis of Cutting Force and Vibration Signals for Tool Condition Monitoring

JUAN C. JÁUREGUI[1], (Senior Member, IEEE), JUVENAL R. RESÉNDIZ[1], (Senior Member, IEEE), SURESH THENOZHI[1], (Member, IEEE), TIBOR SZALAY[2], ÁDÁM JACSÓ[2], AND MÁRTON TAKÁCS[2]

[1]Faculty of Engineering, Autonomous University of Queretaro, Santiago de Queretaro 76010, Mexico
[2]Faculty of Mechanical Engineering, Budapest University of Technology and Economics, 1111 Budapest, Hungary

Corresponding author: Juvenal R. Reséndiz (juvenal@uaq.edu.mx)

This work was supported in part by CONACyT of Mexico through the Bilateral Mexican–Hungarian Project CAR215960 (corresponding Hungarian project number: TÉT_12_MX-1-2013-0015) and in part by PRODEP of Mexico.

ABSTRACT Tool condition monitoring systems are essential in micromilling applications. A tool's slenderness requires high-precision monitoring systems for online measurements. In most cases, tool health is indirectly estimated by processing and analyzing the cutting process parameters. In that sense, the main challenge lies in the proper selection of the process parameters and their processing techniques, so that a robust and accurate assessment of the tool's health is obtained. This paper proposes a frequency- and time-frequency-based analysis of cutting force and vibration signals for estimating the tool condition of a high-speed micromilling process. Measurements obtained from different cutting conditions were utilized in the analysis. The results indicate variations in the dominant frequencies, which result from tool wear. Furthermore, it is important to note that the analysis results obtained from the two process signals provide more reliable results and improve the sensing bandwidth.

INDEX TERMS Condition monitoring, cutting tools, fault detection, micromachining.

I. INTRODUCTION

Micro-milling is a machining process in the frontier of manufacturing small parts for metal-cutting manufacturing processes, where the cutting tool diameters range from 10μm to 800μm and have edge radii that vary from 1μm to 10μm [1]. Different tool types and tool materials have been developed for these applications [2]. However, the demand for higher cutting accuracy and speeds when utilizing such miniature tools can result in a higher risk of tool failure [3]. Tool tip wear, even within microns, can affect the accuracy of micro-milling and the surface finish of the workpiece. Furthermore, these problems can cause delays in the overall manufacturing process. For these reasons, it is necessary to develop certain tool condition monitoring (TCM) systems that can predict the state of the tool. In this way, undesirable consequences, such as tool failure, can be avoided in advance.

Tool condition monitoring can be defined as the process of detecting tool wear and characterizing it. In this process, the process parameters first need to be measured to extract damage-sensitive features. Later, these features are analyzed to determine the current state of tool health. The different stages involved in TCM are shown in Figure 1 and are as follows:

1) *Process Parameters:* Proper monitoring of the process signal is crucial in the TCM process. It is generally classified into two approaches: Direct and Indirect. In the direct method, the tool wear is measured directly; however, it is difficult to provide online monitoring and is generally limited to laboratory setups. Indirect methods are easy to implement and yield more accurate results. They measure the process signals, which are correlated with tool deterioration. A wide range of candidate sensors exist to measure these signals [4].
2) *Signal Processing:* Once the process parameters are sensed, proper pre-processing may be applied based on the signal characteristics. Afterwords, the necessary information for assessing the tool condition needs to be extracted from these signals. The most common types of processing techniques are based on the Time, Frequency and Time-Frequency domain methods [5].

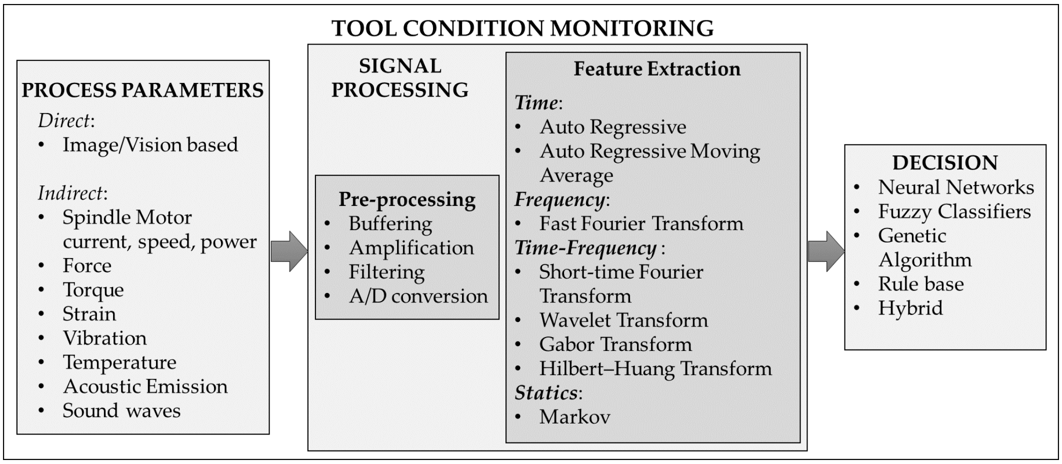

FIGURE 1. Stages involved in the TCM process.

TABLE 1. A summary of the literature reviews on tool condition monitoring for micro-milling applications.

Review	Year	Process parameter	Signal Processing	Decision making
[7]	1997	Direct (Vision based)	-	-
[8]	1997	Indirect	Frequency, Time-Frequency	Neural Networks
[4]	2000	Indirect	-	-
[9]	2002	Indirect (AE)	Time, Frequency, Time-Frequency	Neural Networks, Fuzzy, Group method
[10]	2002	Indirect	Time, Frequency, Time-Frequency	Neural Networks, Rule based, Fuzzy, etc.
[11]	2002	Direct and Indirect	Time, Frequency, Time-Frequency, Statics	Neural Networks
[12]	2005	Indirect	Time, Frequency, Time-Frequency, Statics, Analytical	Neural Networks
[13]	2009	-	Time-Frequency (Wavelets)	-
[14]	2010	Indirect	Frequency, Time-Frequency	Neural Networks, Fuzzy, Fuzzy-Neural Networks
[15]	2010	-	Time, Frequency, Time-Frequency	Neural Networks, Fuzzy, Genetic Algorithm
[16]	2013	Direct (Vision based)	Image Processing	-
[5]	2014	Indirect	Frequency, Time-Frequency	-
[17]	2014	Indirect	Time, Frequency, Time-Frequency, Statics, Entropic Distance method	-

3) *Decision Making:* To gain knowledge about the tool conditions, decision-making methods, such as fuzzy logic and neural networks, may be employed [6]. These algorithms observe the sample corresponding to the tool condition and make a proper decision about the tool health (e.g., tool wear, chipping, breakage, failure and chatter).

Condition monitoring in micro-milling tools is quite challenging. The down-scaling of the process parameters results in significant restrictions during experimental testing, especially in the measurement system. Over the years, a number of studies have been carried out in the field of TCM for micro-milling processes [1], [3], [15]. Due to its popularity and importance, a number of research and review papers and textbooks have been presented. These techniques have been reviewed in a variety of fashions in the literature. The review papers on TCM over the past two decades are summarized in Table 1 and clearly indicate that there is a wide choice of sensors and signal processing techniques that can be utilized for TCM. Most of these tool wear identifications are performed based on information gathered from a single process parameter. To provide reliable detection of the tool condition, multiple process parameters could be incorporated in the analysis. Furthermore, in high-speed machining processes, such as micro-milling operations, the application of multiple sensors increases the sensing frequency bandwidth and improves monitoring accuracy [3]. However, incorporation of multiple parameters can lead to computational complexity or even inaccurate assessments [18]. This necessitates the proper selection of the process parameters and their processing to provide robust and accurate tool condition assessment [19].

Using cutting force is very common in the tool condition monitoring for high-speed milling [20], since it provides a measure of the direct interaction of the tool and the workpiece. However, vibration signal is more sensitive to certain tool wear conditions [21]. The significance of including both the cutting force and vibration signals in tool wear estimation was investigated in [22], and some researchers have included these signals in their analyzes [21], [23]–[25]. In [26], tool failure was detected by measuring the increase in the cutting force and vibration amplitude via frequency response analysis. In [27], the bandwidth limitation of the force sensor was overcome by incorporating an accelerometer during the measurement utilizing an expanded Kalman Filter, which incorporates both the force and vibration signals to reconstruct the high-frequency bandwidth cutting forces from the distorted cutting force measurements.

To improve tool wear detection, especially at higher frequencies, some researchers have utilized Acoustic Emission (AE) signal along with the cutting force and vibration signals [22], [28]. Tool wear estimation based on a neuro-fuzzy model was studied in [3], which indicates that an estimation using only the force signal was shown to be less accurate due to bandwidth limitations. This drawback is overcome by adding the acceleration and AE sensor, which increased the measurement bandwidth required to capture more features related to tool wear. In [19], sensor fusion of the force, vibration, and machine acoustic signals was performed using a fuzzy model for effective tool wear prediction. The authors also reported that the performance of the multiple sensors for detecting the tool wear is better compared to a single parameter case. However, AE can generate high-frequency noise signals [22].

Once the process parameter has been sensed, an appropriate signal processing technique needs to be applied to extract the necessary information related to the tool condition. There exist different signal processing methods, which are highly subjective in nature and very specific for the application at hand. The Fast Fourier Transform (FFT) is the most widely used signal analysis method. The FFT is not very useful for analyzing nonlinear, transient or non-stationary signals, as it does not describe the frequency content of a signal at specific times. A time-frequency analysis can describe the process signal features in both time and its corresponding frequency. This can help in determining localized features related to the tool condition [13], [21]. The Short-time Fourier Transform (STFT) is a time-dependent Fourier transform, which maps a signal into a two-dimensional function of time and frequency. It is computed using a sliding window with fixed length. The performance of the STFT mainly depends on the type and length of the chosen window. As per the Heisenberg inequality, a fixed window length results in a constant product of time and frequency resolutions, resulting in a trade-off, where it is not possible to achieve good time and frequency resolution simultaneously. Thus, an improved processing method is required, and the Wavelet Transform may be a better alternative. Compared to the STFT, the multi-resolution capability of the Wavelet Transform provides a balance between time and frequency resolution: the time resolution becomes better at higher frequencies, whereas the frequency resolution becomes better at lower frequencies [13].

The main objective of this paper is to choose the proper process parameters and their processing techniques. In that way, the health of the tool can be estimated accurately. The cutting force and vibration signals are widely utilized in estimating the tool condition. This paper proposes a methodology for tool wear assessment by performing simultaneous measurements of the force and vibration signals and analyzing them with frequency and time-frequency techniques. The tool wear is detected from a design of the experiment including different tools and cutting conditions. In this work, only the results for one tool are included to demonstrate the robustness of the proposed method. The tool wear estimation is obtained by the simultaneous analysis of the FFT and Continuous Wavelet Transform (CWT) and the variations in frequency, amplitude, and the presence of nonlinear responses as the cutting advances. A combination of the force and vibration signals and FFT and CWT techniques provides a robust and accurate tool wear assessment.

II. PROPOSED APPROACH

The proposed approach is to diagnose the tool wear by performing simultaneous measurements of the force and vibration signals and then analyzing them with frequency and time-frequency techniques. The steps involved in the proposed approach are as follows:

1) *Experiments:* Various experiments under the different cutting conditions will be conducted on a micro-milling center, and the corresponding cutting force and vibration signals during the cutting process will be measured simultaneously.
2) *Tool Analysis:* Here, the natural frequency of the micro tool and the corresponding Insert Passing Frequency (IPF) for the cutting conditions will be obtained.
3) *Signal Analysis:* Frequency and time-frequency analysis techniques will be employed to extract the parameters corresponding to the tool wear.
4) *Tool Wear Estimation:* Based on the frequency and time-frequency analyzes, the tool wear is estimated by detecting variations in the frequency, amplitude, and presence of any nonlinear responses during the cutting process.

A detailed discussion of the aforementioned methodologies will be provided in the following subsections.

A. DESIGN OF EXPERIMENTS

From the present review, we seen that the cutting forces and vibration signals are the most widely utilized parameters in TCM. Accelerometers are generally used to measure the vibration generated during the tool-workpiece interaction. However, during the cutting process, additional vibration signals can be generated by the machine itself, such as 1) the

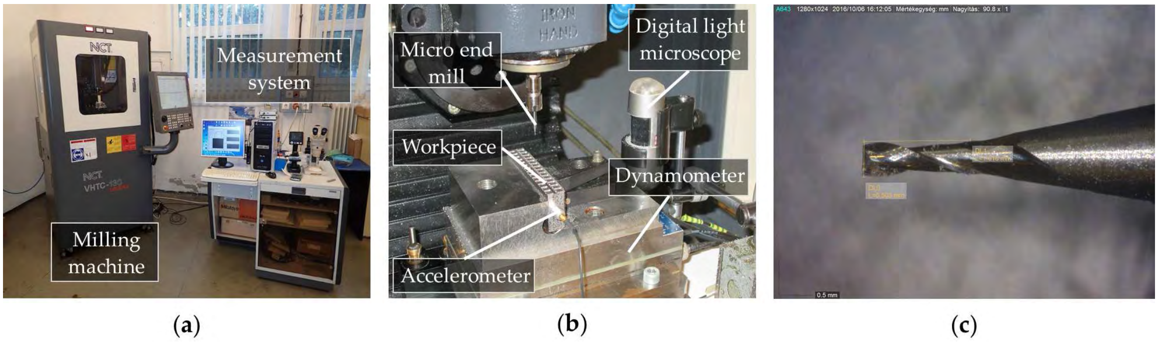

FIGURE 2. Experimental setup: (a) Micro-milling machine with measurement system, (b) Fixed micro end mill together with the workpiece on the Kistler dynamometer and the piezoelectric accelerometer, and (c) Magaforce micro tool.

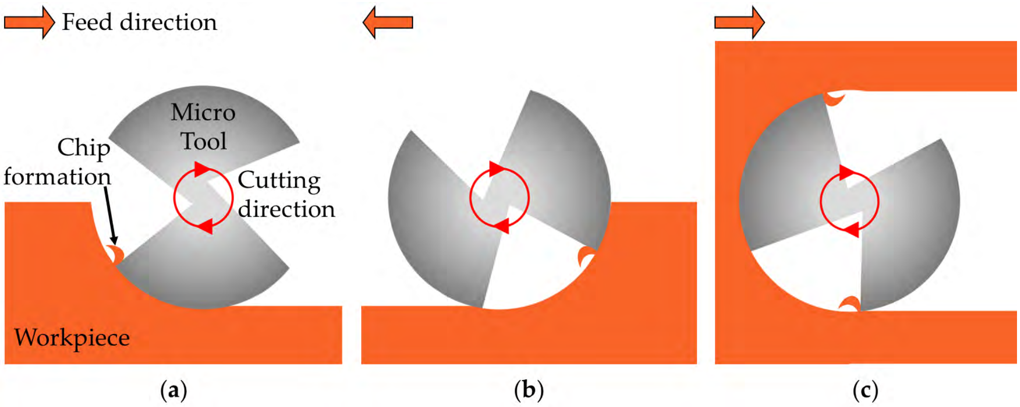

FIGURE 3. Types of milling operations based on the cutting direction of the tool with respect to the feed direction of the workpiece: (a) Up-milling, (b) Down-milling, and (c) Full-milling.

spindle generating vibrations at the rotating frequency and its harmonics, even when there is no cutting; 2) misalignment generating vibrations that occur at higher harmonics of the rotating frequency; and 3) other synchronous and non-synchronous frequencies that are always present. All these vibrations are sensed by the accelerometer along with vibrations caused by the tool-workpiece interactions, which occur at the same frequency as some of the machine excitation frequencies. This condition causes difficulty in extracting features related to tool wear. Since the force sensor measures the force only during the tool-workpiece interaction and no other signals, it provides a higher signal-to-noise ratio and easy isolation of the forces acting on the different cutting directions. Nevertheless, it cannot record high-frequency signals. In terms of frequency, the accelerometer provides a higher measurement bandwidth than the force sensor. In this study, we use both force (3-axis) and vibration (1-axis) sensors to leverage the advantages of both measurements.

The experimental cutting tests are performed at the micro-milling center (Model: NCT VHTC-130M) at the Department of Manufacturing Science and Engineering at the Budapest University of Technology and Economics. The experimental setup used to detect the state of the tool in the milling process is shown in Figures 2 (a) and (b). A piezoelectric accelerometer (Model: Brüel & Kjaer 4518-001) and a 3-axis force dynamometer (Model: Kistler 9257A) were employed to measure the vibration and cutting force signal, respectively. These signals were acquired simultaneously using an NI USB-4431 data acquisition system at sampling frequencies in the range from 38, 200Hz and 89, 100Hz. High efficiency shielded cables are used to reduce noise.

The workpiece material used in this work is AISI 1045, and the experiments are performed using different micro tools (Magaforce, Fraisa, Seco). This paper only consider the analysis of experiments obtained using the Magaforce tool (manufactured by Magafor), which is a two-flute solid carbide uncoated milling tool with a diameter of 0.5mm and length of 1.6mm; see Figure 2 (c).

Based on the rotation direction of the cutting tool and the feed direction of the workpiece, the milling operation can have different configurations. This paper considers Up-milling, Down-milling and Full-milling operations, as shown in Figure 3. To study the tool wear mechanism, the cutting operations were initiated with a new tool and continued until a tool breakage is identified. For that purpose, tool snapshots were taken to measure the amount of tool wear after each set of cutting processes, as shown in Figure 4. A total of 15 experimental tests (Test 1 was performed using

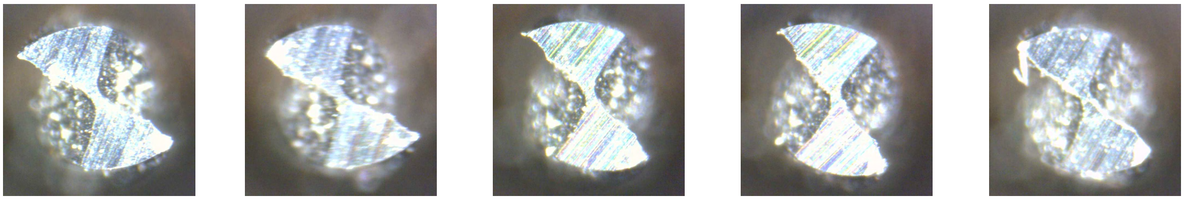

(a) (b) (c) (d) (e)

FIGURE 4. Snapshots of the Magaforce tool obtained after each set of cutting processes: (a) Tests 1-3 (New tool), (b) Tests 4-6, (c) Tests 7-9, (d) Tests 10-12, and (e) Tests 13-15 (Broken edge).

TABLE 2. Summary of the cutting conditions.

No.	Dir.	v_c (m/min)	f_z (μm)	a_p (mm)	n (rpm)
1.	Up	60	2	0.05	38197
2.	Full	60	2	0.05	38197
3.	Down	60	2	0.05	38197
4.	Up	90	2	0.05	57296
5.	Full	90	2	0.05	57296
6.	Down	90	2	0.05	57296
7.	Up	40	4	0.05	25465
8.	Full	40	4	0.05	25465
9.	Down	40	4	0.05	25465
10.	Up	90	4	0.05	57296
11.	Full	90	4	0.05	57296
12.	Down	90	4	0.05	57296
13.	Up	40	1	0.05	25465
14.	Full	40	1	0.05	25465
15.	Down	40	1	0.05	25465

the new tool and a broken edge was found after Test 15) were conducted at various cutting speeds, feed rates and cutting directions (Up, Down and Full). The details of the cutting conditions, such as direction of cutting (Dir.), cutting speed (v_c), feed rate per edge (f_z), depth of cut (a_p), and spindle speed (n), used for each test are summarized in Table 2.

B. TOOL ANALYSIS

The Magaforce tool used in the experiments is relatively slender and can have large deformations. For this reason, the natural frequencies were estimated using a large deformation model [29]:

$$m\frac{d^2w}{dt^2} + EI\left(\frac{1485w^5}{385l^7} - \frac{162w^3}{35l^5} + \frac{3w}{l^3}\right) = f(t) \quad (1)$$

where m is the mass, E is the elastic modulus, I is the moment of inertia, l is the tool length, w is the displacement, and $f(t)$ is the excitation force.

Since (1) is nonlinear, the natural frequency of the cutting tool can be calculated via numerical simulations by exciting the system with an impulse input, i.e., $f(t) = \delta(t)$. The corresponding frequency spectrum for the Magaforce tool is shown in Figure 5. From the spectrum, its natural frequency was determined to be 65, 302Hz. Since the experiment measurement range is only as high as 15, 000Hz, the tool's natural frequency would not affect the analysis results.

Another important parameter in tool health estimation is the IPF. This is a critical parameter for identifying the cutting

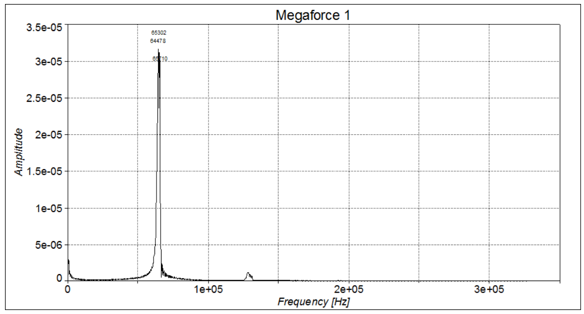

FIGURE 5. Deformation model based frequency response of the Magaforce tool.

frequency from the rest of the vibration sources. The IPF is decided by the number of edges in the cutting tool, which can be calculated from:

$$\mathrm{IPF} = \frac{nz}{60} \quad (\mathrm{Hz}) \quad (2)$$

where z is the number of edges in the cutting tool. The Magaforce tool contains two cutting edges, hence $z = 2$.

C. SIGNAL ANALYSIS

For determining the tool condition, both the cutting force and vibration signals were analyzed with signal processing techniques. This information is difficult to understand just from the original data, meaning it must be processed. For this purpose, the frequency (FFT) and time-frequency (CWT) analysis techniques were applied. Since the FFT is a well-known technique, its description is outside of the scope of this paper. Meanwhile, the CWT is described for a better understanding of its application in the TCM.

The wavelet transform is used to obtain a two-dimensional representation, termed as the spectrogram or time-frequency map of a one-dimensional signal. The advantage of these maps is the separation of individual frequencies as a function of time. The CWT, $X(s, \tau)$ of the signal $x(t)$ can be obtained by performing the continuous convolution of the wavelet function with the signal over the entire continuum of wavelet scales:

$$X(s, \tau) = \langle x(t)|\,\psi(s, \tau)\rangle = \frac{1}{\sqrt{s}}\int_{-\infty}^{\infty} x(t)\psi^*\left(\frac{t-\tau}{s}\right)\mathrm{d}t \quad (3)$$

where $s > 0$ is the scaling factor, which is inversely proportional to the frequency, τ is the time shifting factor, $\langle x(t)|\,\psi(s,\tau)\rangle$ indicates the inner product or the projection of the signal $x(t)$ onto the mother wavelet function $\psi(s,\tau)$, and ψ^* is the complex conjugate of ψ. In this manner, a one-dimensional signal is represented as a two-dimensional function, separating the original signal into a set of signals of different frequencies.

A large selection of mother wavelets is available for different applications. The Morlet wavelet function is a good candidate for the feature extraction applications, as it provides a good balance between time and frequency resolutions [30]. The Morlet wavelet function is used as the mother wavelet in our analysis, which is formed by a sinusoidal function and a logarithm decrement function, defined as:

$$\psi\left(\frac{t-\tau}{s}\right) = \mathrm{e}^{i2\pi f_0\left(\frac{t-\tau}{s}\right)}\mathrm{e}^{-\alpha\frac{(t-\tau)^2}{s^2\beta^2}} \tag{4}$$

where f_0 is the frequency of the sinusoidal function and α and β are constants. This function has a similar "shape" as the response of a stable linear system. By varying the wavelet parameters s and τ, the wavelet transform decomposes a given signal into a time series along the entire spectrum. Here, the small-scale factors decompose high-frequency components, whereas large-scale factors decompose low-frequency components.

In the analysis of nonlinear dynamics, the wavelet transform can be useful to discriminate the frequencies that remain constant along the entire response from those that vary with time. The constant frequencies are related to a linear behavior, whereas the varying frequencies are related to nonlinear behavior.

Once the force and vibration signals are measured from the experiments, the following analyzes extract the information related to tool wear:

1) The presence of harmonic and non-harmonic components and their amplitudes will be obtained by transforming the signals into the frequency domain using FFT. This will also provide information about the frequency band where signal processing needs to be applied.
2) Since the time information is lost during the frequency transformation, it is impossible to separate the harmonics related to the machine and the cutting process. This drawback is overcome by performing a time-frequency analysis using CWT. From the time-frequency map, the frequency components that appear only during the cutting process and entire machine operations will be separated.
3) To study the nature of the cutting process, the CWT will be further used to identify the frequency components that vary with time. In that case, it is assumed that the behavior at those frequencies is nonlinear. However, if the frequency components remain constant, the behavior is linear.

D. TOOL WEAR ESTIMATION

The tool wear estimation is obtained by a simultaneous analysis of the FFT and CWT for identifying vibration frequencies, amplitudes and the presence of any nonlinear responses. In this work, the following criteria are considered:

1) The behavior of IPF (1×IPF) and its *harmonic* frequencies (2×IPF, 3×IPF).
2) The presence of non-harmonic frequencies at exact fractions of the IPF (0.5×IPF, 1.5×IPF, 2.5×IPF) and the presence of non-harmonic frequencies that are not a fraction of the IPF.
3) The level of nonlinearity, in terms of amplitude, as the cutting process advances.

In the case of a healthy tool, the harmonic and non-harmonic components will appear at the *nominal frequencies* (1×IPF, 2×IPF, 3×IPF and 0.5×IPF, 1.5×IPF, 2.5×IPF, respectively). As the tool is worn, there will be non-harmonic frequencies, which are not at exact fractions of IPF that appear at new frequencies. The main goal of the FFT and CWT analysis is to identify those frequencies, as the low friction due to the tool-workpiece interaction always generates non-harmonic frequencies at 0.5×IPF, 1.5×IPF, 2.5×IPF for a healthy cutting condition.

III. RESULTS AND DISCUSSION

The cutting force and vibration signals were measured simultaneously to determine the tool wear for up, full and down milling operations. The measured signals were detrended, where the mean value of each measurement was subtracted and normalized. To analyze the tool condition, both the FFT and CWT analyzes conducted on both the cutting force and vibration data were performed using the AutoSignal ™1.7 (SeaSolve Software, Inc.) software package. The software is configured to use the Radix-2 method for the FFT analysis and Morlet wavelet for the CWT analysis. Based on these analyzes, the dominant features were obtained to predict the tool condition. In all cases, a full discussion of the results is carried out and presented below.

A. ANALYSIS OF CUTTING FORCE SIGNAL

In this study, the relationship between the tool wear and cutting force in three axes (F_x, F_y, F_z) is discussed. The analysis is performed for a frequency range of 0Hz to 5, 000Hz. During the analysis, several aspects were taken into consideration: the ratio between the dominant frequencies versus the IPF or cutting frequency, the ratio between the IPF amplitudes in each direction, and the most significant nonlinearities.

As an example, the cutting force signal in the x-direction (F_x) obtained from Test 1 is shown in Figure 6. Figure 6 (a) shows the original measured data obtained from the force sensor. From this, we see that cutting occurs from 6.6s to 8.6s. The measured signal is then detrended, and the FFT analysis is performed, as shown in Figure 6 (b). This gives the dominant frequencies and their corresponding amplitudes. The cutting is performed with a spindle speed of $n = 38,197$rpm, i.e., $N = n/60 = 636$Hz. Using (2), the IPF is calculated to

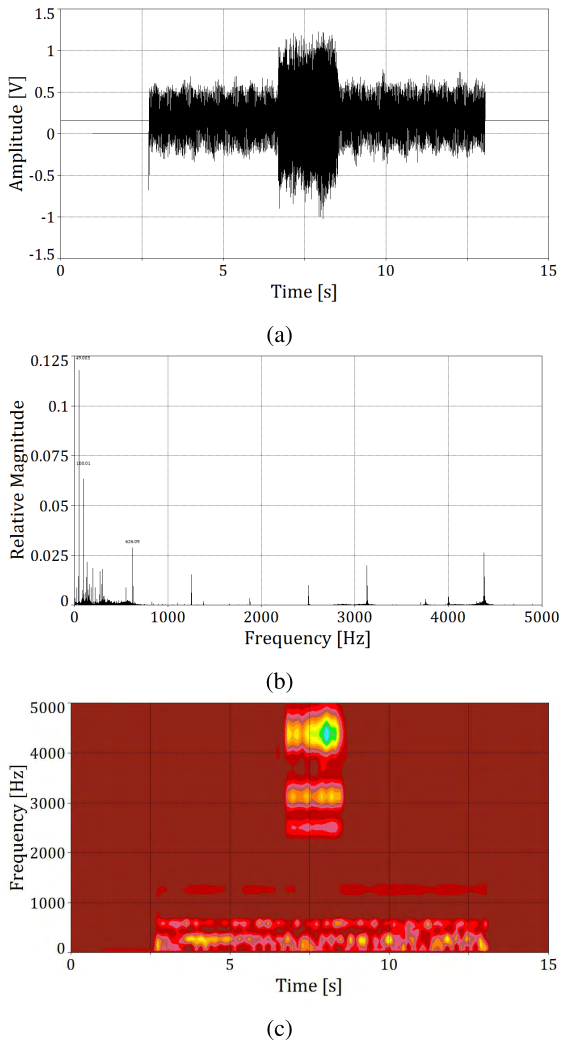

FIGURE 6. Representations of the force signal (F_X) obtained for Test 1: (a) Time-domain, (b) Frequency-domain (FFT), and (c) Time-Frequency (CWT).

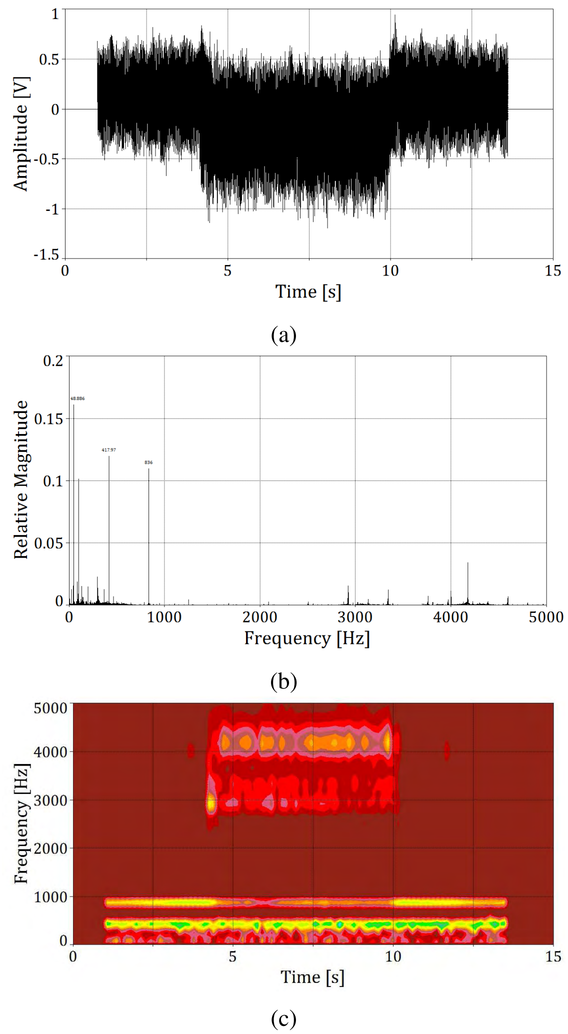

FIGURE 7. Representations of the force signal (F_X) obtained for Test 15: (a) Time-domain, (b) Frequency-domain (FFT), and (c) Time-Frequency (CWT).

be $1,272$Hz, which is $2N$. Similar to the FFT analysis, peaks can be seen at 626Hz and $1,252$Hz, which is close to the calculated values. Finally, using the CWT, a time-frequency map is obtained, which is shown in Figure 6 (c). Using this map, the frequency peaks occurring during the cutting period and the entire machine process are separated. In this case, the frequencies $2,504$Hz, $3,130$Hz and $4,383$Hz appear only during the cutting period from $6.6s$ to $8.6s$, whereas the frequencies 626Hz, $1,252$Hz and $1,878$Hz appear during the entire measurement, meaning they are related to machine operations.

The same analysis is performed on the signals obtained from the entire test conditions (Tests 1-15), with the corresponding results summarized in Table 3 showing the most dominant frequency peaks at three orthogonal directions and their ratios with respect to the IPF. It also includes the amplitude of the IPF in each direction and its ratio with respect to F_x. The CWT analysis results were used to separate the frequency components during cutting and machine operations. The frequencies indicated with blue colored bold fonts represent the frequencies related to the cutting process only.

B. ANALYSIS OF VIBRATION SIGNAL

Similar to the force signal analysis, FFT and CWT analyzes were performed on the vibration signals over a frequency range from 0Hz to $15,000$Hz. An example of the vibration signal (Test 1) and the corresponding FFT and CWT analyzes results are shown in Figure 8. Table 4 shows the analysis results of the vibration signal obtained for Tests 1-15 with the most dominant frequency peaks and its ratio with respect to the IPF. The frequencies related to the cutting process are indicated with blue-colored bold fonts.

Apart from providing a reliable analysis from 0Hz to $5,000$Hz, the acceleration measurement can be used to improve the tool wear detection capability by capturing the cutting process features at higher frequencies.

TABLE 3. Time-frequency analysis of cutting force signal.

No.	Frequency (Hz)																					Amplitude		
	F_x						F_y						F_z									F_x	F_y	F_z
$N = 636$, $IPF = 1272$, see Figure 4: (a)																								
1.	626	1252	1878	**2504**	**3130**	**4383**	626	1252	**1878**	**2504**	**3130**	**3757**	626	1252	1878	**3130**	3757	4002	**4383**	-	-	0.02	0.02	0.13
	0.49	0.98	1.48	1.97	2.46	3.45	0.49	0.98	1.48	1.97	2.46	2.95	0.49	0.98	1.48	2.46	2.95	3.15	3.45	-	-	1.00	1.07	8.47
2.	626	1252	1878	**2504**	**3124**	**4383**	626	1252	**1878**	2504	**3130**	**3757**	626	1252	1381	1878	3757	4002	**4383**	-	-	0.02	0.01	0.15
	0.49	0.98	1.48	1.97	2.46	3.45	0.49	0.98	1.48	1.97	2.46	2.95	0.49	0.98	1.09	1.48	2.95	3.15	3.45	-	-	1.00	0.67	8.56
3.	626	1252	**1878**	**2504**	**3130**	**4383**	626	1252	**1878**	**2504**	**3130**	**3757**	626	1252	1878	**3130**	3757	4002	**4383**	-	-	0.02	0.01	0.15
	0.49	0.98	1.48	1.97	2.46	3.45	0.49	0.98	1.48	1.97	2.46	2.95	0.49	0.98	1.48	2.46	2.95	3.15	3.45	-	-	1.00	0.55	7.55
$N = 954$, $IPF = 1908$, see Figure 4: (b)																								
4.	416	830	**2865**	**3820**	-	**4660**	416	-	**1910**	**2865**	**3820**	-	416	830	938	1250	**1910**	**2865**	**3820**	4000	**4660**	0.008	0.014	0.03
	0.22	0.43	1.50	2.00	-	2.44	0.22	-	1.00	1.50	2.00	-	0.22	0.43	0.49	0.65	1.00	1.50	2.00	2.09	2.44	1	1.75	3.75
5.	415	938	**2860**	**3820**	4000	-	415	938	**1910**	**2860**	**3820**	-	415	-	938	1250	**1910**	**2860**	**3820**	-	**4660**	0.008	0.035	0.03
	0.22	0.49	1.50	2.00	2.09	-	0.22	0.49	1.00	1.50	2.00	-	0.22	-	0.49	0.65	1.00	1.50	2.00	-	2.44	1	4.375	3.75
6.	415	938	**2860**	**3820**	-	4660	415	938	**1910**	**2860**	**3820**	4000	415	-	938	1250	**1910**	**2860**	**3820**	4000	**4660**	0.009	0.02	0.055
	0.22	0.49	1.50	2.00	-	2.44	0.22	0.49	1.00	1.50	2.00	2.09	0.22	-	0.49	0.65	1.00	1.50	2.00	2.09	2.44	1	2.222	6.111
$N = 424$, $IPF = 848$, see Figure 4: (c)																								
7.	416	833	1950	**2850**	**4160**	-	416	833	-	-	**3330**	-	416	833	-	**1270**	1950	-	-	4000	**4160**	0.13	0.10	0.72
	0.49	0.98	2.30	3.36	4.90	-	0.49	0.98	-	-	3.92	-	0.49	0.98	-	1.50	2.30	-	-	4.71	4.90	1.00	0.77	5.54
8.	-	833	1950	-	-	-	416	833	-	-	**3330**	-	416	833	-	**1270**	1950	-	-	**4000**	-	0.11	0.80	0.68
	-	0.98	2.30	-	-	-	0.49	0.98	-	-	3.92	-	0.49	0.98	-	1.50	2.30	-	-	4.71	-	1.00	7.27	6.18
9.	416	833	1950	**3330**	**4160**	-	416	833	**1250**	**1950**	**2850**	3660	416	833	-	**1250**	1950	-	-	**4000**	-	0.13	0.09	0.77
	0.49	0.98	2.30	3.92	4.90	-	0.49	0.98	1.47	2.30	3.36	4.31	0.49	0.98	-	1.47	2.30	-	-	4.71	-	1.00	0.72	6.16
$N = 954$, $IPF = 1910$, see Figure 4: (d)																								
10.	416	-	938	**2850**	**3750**	**4660**	416	-	**1650**	-	**2850**	**3750**	416	833	938	1250	1650	**2850**	**3820**	4000	**4660**	0.04	0.02	0.03
	0.22	-	0.49	1.49	1.96	2.44	0.22	-	0.86	-	1.49	1.96	0.22	0.44	0.49	0.65	0.86	1.49	2.00	2.09	2.44	1.00	0.50	0.75
11.	416	938	**1900**	**2850**	**3750**	4000	-	938	**1900**	-	-	**3750**	-	-	938	-	**1900**	**2850**	-	4000	-	0.01	0.03	0.04
	0.22	0.49	0.99	1.49	1.96	2.09	-	0.49	0.99	-	-	1.96	-	-	0.49	-	0.99	1.49	-	2.09	-	1.00	3.00	4.00
12.	-	-	-	**2850**	**3750**	**4660**	416	938	**1900**	**2850**	**3850**	4000	416	833	1250	-	**1900**	**2850**	**3850**	4000	**4660**	0.02	0.02	0.05
	-	-	-	1.49	1.96	2.44	0.22	0.49	0.99	1.49	2.02	2.09	0.22	0.44	0.65	-	0.99	1.49	2.02	2.09	2.44	1.00	1.60	3.60
$N = 424$, $IPF = 848$, see Figure 4: (e)																								
13.	416	**832**	-	**2850**	-	**4250**	416	**832**	-	**2850**	**3850**	-	416	**833**	-	-	-	-	-	4000	**4250**	0.13	0.11	0.75
	0.49	0.98	-	3.36	-	5.01	0.49	0.98	-	3.36	4.54	-	0.49	0.98	-	-	-	-	-	4.71	5.01	1.00	0.85	5.77
14.	416	**833**	-	**2850**	4000	**4250**	416	**833**	**1700**	**2550**	**3820**	4000	416	**833**	-	-	-	-	-	4000	-	0.08	0.07	0.07
	0.49	0.98	-	3.36	4.71	5.01	0.49	0.98	2.00	3.00	4.50	4.71	0.49	0.98	-	-	-	-	-	4.71	-	1.00	0.93	0.87
15.	416	**833**	**1270**	**2550**	4000	**4250**	416	**833**	**1270**	**2550**	**3820**	4000	416	**833**	**1270**	-	-	-	-	4000	-	0.12	0.08	0.70
	0.49	0.98	1.50	3.00	4.71	5.01	0.49	0.98	1.50	3.00	4.50	4.71	0.49	0.98	1.50	-	-	-	-	4.71	-	1.00	0.70	6.09

TABLE 4. Time-frequency analysis of vibration signal.

No.	Frequency (Hz)																			
$N = 636$, $IPF = 1272$, see Figure 4: (a)																				
1.	626	1252	1879	2504	**3130**	3758	**4363**	5637	6242	**7513**	8121			10606	11880				13759	14363
	0.49	0.98	1.48	1.97	2.46	2.95	3.43	4.43	4.91	5.91	6.38			8.34	9.34				10.82	11.29
2.	626	1252	1879			3758	**4383**	5636	6242	**7515**	8121				11880	12180			13759	14363
	0.49	0.98	1.48			2.95	3.45	4.43	4.91	5.91	6.38				9.34	9.58			10.82	11.29
3.	626	1252	1878	2504	**3130**	3758	4383	5636	6262	**7515**	8141	8766	9393	10646	11898		12525	13151	13759	14363
	0.49	0.98	1.48	1.97	2.46	2.95	3.45	4.43	4.92	5.91	6.40	6.89	7.38	8.37	9.35		9.85	10.34	10.82	11.29
$N = 954$, $IPF = 1908$, see Figure 4: (b)																				
4.	415	830	938	1878	**2815**	**3754**	**4962**	**5630**	6569	7182	**7507**	8446	**9384**	10323	**11262**	12200	12819	13139	14075	
	0.22	0.44	0.49	0.98	1.48	1.97	2.60	2.95	3.44	3.76	3.93	4.43	4.92	5.41	5.90	6.39	6.72	6.89	7.38	
5.	415	830	938	1877	**2815**	**3754**	**4962**	**5631**	**6570**	7182	**7508**		**9385**	10324			12818	13139		
	0.22	0.44	0.49	0.98	1.48	1.97	2.60	2.95	3.44	3.76	3.94		4.92	5.41			6.72	6.89		
6.	415	830	938	1876	**2815**	**3754**	**4962**	**5630**		7182	**7508**	8445	**9384**	10323	**11261**	12200	12819	13138		
	0.22	0.44	0.49	0.98	1.48	1.97	2.60	2.95		3.76	3.94	4.43	4.92	5.41	5.90	6.39	6.72	6.89		
$N = 424$, $IPF = 848$, see Figure 4: (c)																				
7.	414	450	675	827	936	1125	1874	2812	**3750**	5623	5643	**6560**	**7497**	8434	9372	10310	**11287**	**12185**	13124	14059
	0.49	0.53	0.80	0.98	1.10	1.33	2.21	3.32	4.42	6.63	6.65	7.74	8.84	9.95	11.05	12.16	13.31	14.37	15.48	16.58
8.	413	450	675	828	938	1125	1575	1875	2821	3376	4967	5643	**6560**	8465	**10310**	11287	12185	13122	14037	
	0.49	0.53	0.80	0.98	1.11	1.33	1.86	2.21	3.33	3.98	5.86	6.65	7.74	9.98	12.16	13.31	14.37	15.47	16.55	
9.	450	675	938	1125	1575	1874	2811	3376	5623	5643	**6561**	7499	8465	9373	**10311**	11287	12186	13124	14037	14108
	0.53	0.80	1.11	1.33	1.86	2.21	3.31	3.98	6.63	6.65	7.74	8.84	9.98	11.05	12.16	13.31	14.37	15.48	16.55	16.64
$N = 954$, $IPF = 1910$, see Figure 4: (d)																				
10.	415	830	938	1878	**2815**	**3754**	**4692**	**5631**	**6570**	7182	**7509**	8447	**9385**	10324	11263		12819	13140	14079	14365
	0.22	0.43	0.49	0.98	1.47	1.97	2.46	2.95	3.44	3.76	3.93	4.42	4.91	5.41	5.90		6.71	6.88	7.37	7.52
11.	415	830	**938**	1878	**2815**	**3754**	**4692**	**5631**	**6569**	7182	**7509**	8446	**9345**	10323			12818	13142		14365
	0.22	0.43	0.49	0.98	1.47	1.97	2.46	2.95	3.44	3.76	3.93	4.42	4.89	5.40			6.71	6.88		7.52
12.	415	830	**938**	1878	**2815**	**3754**	**4692**	**5630**	**6569**	7182	**7507**	8446		10323	11262	12200	12818	13138	14077	14365
	0.22	0.43	0.49	0.98	1.47	1.97	2.46	2.95	3.44	3.76	3.93	4.42		5.40	5.90	6.39	6.71	6.88	7.37	7.52
$N = 424$, $IPF = 848$, see Figure 4: (e)																				
13.	415	450	674	830	940	1124	1573	1880	2820	3372	5643	**6581**	7522	8465	9403	**10343**	11287	13164	14037	14105
	0.49	0.53	0.79	0.98	1.11	1.33	1.85	2.22	3.33	3.98	6.65	7.76	8.87	9.98	11.09	12.20	13.31	15.52	16.55	16.63
14.	415	450	675	830	940	1124	1573	1880	2820	3373	4968	5643	**6581**	7522	8464	9405	**10344**	11287	14037	14108
	0.49	0.53	0.80	0.98	1.11	1.33	1.85	2.22	3.33	3.98	5.86	6.65	7.76	8.87	9.98	11.09	12.20	13.31	16.55	16.64
15.	415	450	675	830	940	1124	1574	1880	2821	3375	4968	5643	**6583**	7523	8464	9404	**10345**	11287	13167	14036
	0.49	0.53	0.80	0.98	1.11	1.33	1.86	2.22	3.33	3.98	5.86	6.65	7.76	8.87	9.98	11.09	12.20	13.31	15.53	16.55

C. DISCUSSION

To measure the tool wear, the behavior of the harmonic and non-harmonic frequencies present in both the cutting force and vibration signal was analyzed.

According to the tool shape, the force function produces a vibration at the IPF (twice the rotating speed) due to the presence of the two cutting edges. In the case of the cutting force analysis, there are more frequencies in the F_z direction,

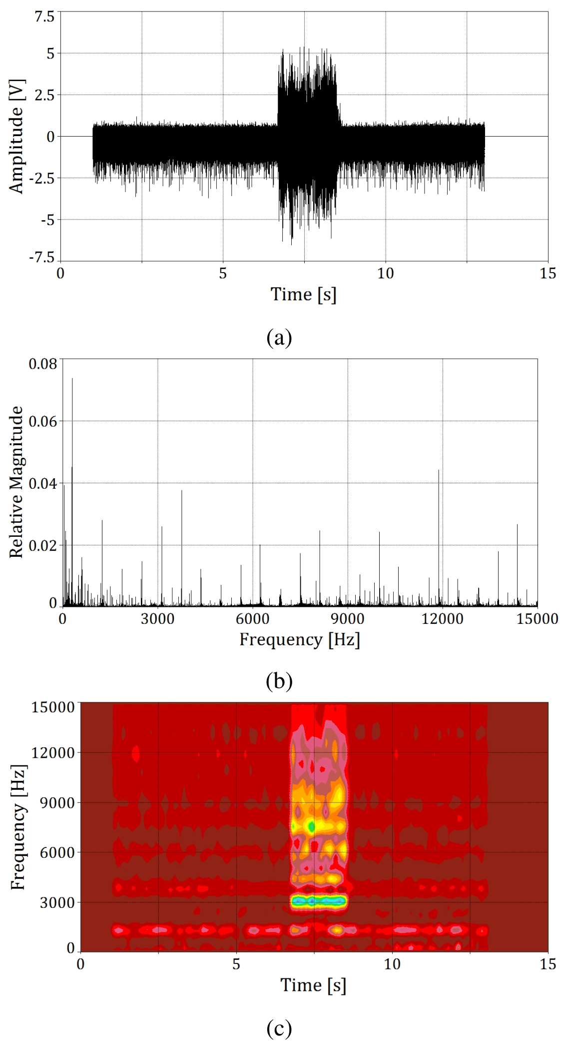

FIGURE 8. **Representations of the vibration signal obtained for Test 1: (a) Time-domain, (b) Frequency-domain (FFT), and (c) Time-Frequency (CWT).**

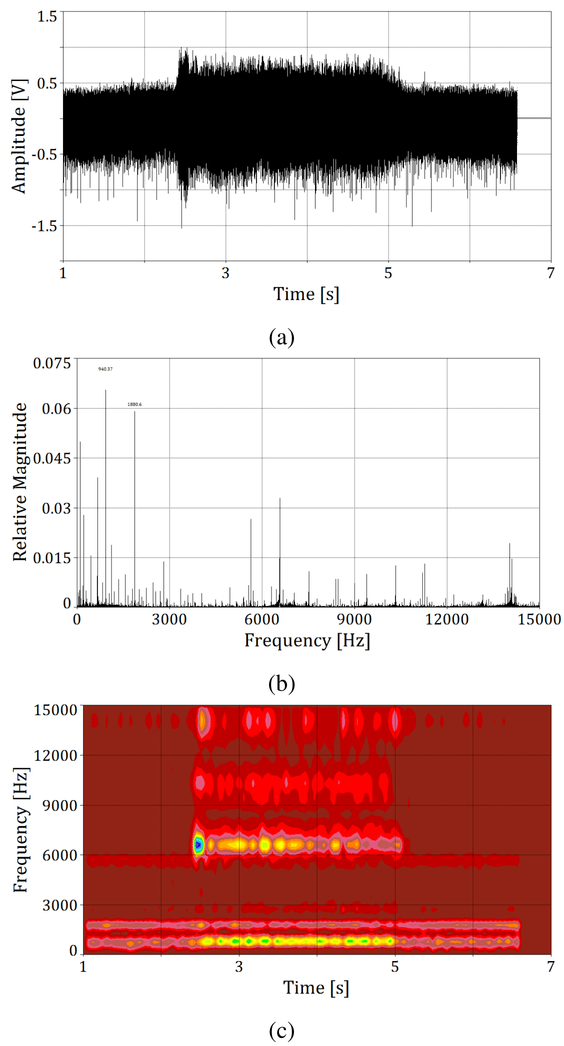

FIGURE 9. **Representations of the vibration signal obtained for Test 15: (a) Time-domain, (b) Frequency-domain (FFT), and (c) Time-Frequency (CWT).**

as shown in Table 3. It is noted that there are non-harmonic frequencies at 0.5×IPF, 1.5×IPF, 2.5×IPF. This may be the effect of the friction force generated by axial contact between the non-cutting insert and the workpiece. The tool wear information in the force signals appears to be contained in the high-frequency components and in few low-frequency components.

A closer inspection shows that in the case of a healthy tool, the harmonic and non-harmonic components are well defined at the nominal frequencies. In all the tests, there is a peak at 4, 000Hz that is not related to any process condition but in most cases synchronizes with the 2×IPF. As the cutting process advances, it is noted that some of these frequencies are either shifted or even absent. For the non-harmonic case, this indicates that the high friction caused by the wear tool surface results in such deviations. For the case of F_x, the analysis results from Tests 7-9 and 11 for the 2.5×IPF is shifted to 2.3×IPF. For Tests 13-15, this non-harmonic component is not present due to tool breakage. This is visible in Figure 4 (e) where a broken edge is observed after Test 15. The corresponding FFT and CWT analysis results are shown in Figure 7.

The above observation is more evident from the analysis of the vibration signals. To perform a fair comparison between the cutting force and vibration signal, we restrict the vibration frequencies less than 5, 000Hz. For Tests 1-3, we note that the harmonic and non-harmonic components are clearly present in the nominal frequencies. For Tests 13-15, it is noted that new frequency components are introduced at 0.53×IPF, 0.8×IPF, and 1.11×IPF and its harmonics, 1.33×IPF and 1.86×IPF. For a better understanding, the FFT and CWT analysis results from the vibration signal obtained for Test 15 are provided in Figure 9.

The behavior of the amplitude ratio, in terms of IPF, of the cutting force in the three orthogonal directions was studied using FFT; see Table 3. The main objective was to determine if the ratio of the amplitudes varied with respect to tool wear. In other words, it was expected that the amplitude ratio varies linearly as the tool wear advances. However, the results do not show any conclusive evidence to relate these phenomena. Next, the relationship between tool wear and the level of nonlinearity in the harmonic and non-harmonic frequencies during the cutting process (indicated in blue-colored bold fonts) was analyzed using CWT. In this case, the objective was to check if the level of nonlinearity varied as the tool wear advances. Here, the level of nonlinearity implies the continuity or variation in amplitudes at each dominant frequency. For example, the amplitude remaining constant during the cutting process implies that a particular frequency is linear in nature. However, if the amplitude is varying or discontinuous, it indicates a strong nonlinearity. In this study, the time-frequency analysis was utilized. As an example, for a force signal (F_x) obtained for Test 1, the frequency at $3,130$Hz is more nonlinear compared to the frequency at $2,504$Hz, as shown in Figure 6 (c). However, from the CWT analysis of both the force and vibration signals from Tests 1-15, there was insufficient evidence to identify a relationship between the nonlinearity level and tool wear, as the nonlinearity levels remained relatively unchanged, and only the non-harmonic frequencies were shifted from the nominal values.

IV. CONCLUSION

This paper presents a methodology for the detection of tool wear based on frequency and time-frequency analysis of the cutting force and vibration signals. First, experiments were carried out on a micro-milling center using different cutting conditions, and the corresponding cutting force and vibration signals were measured simultaneously. Second, using FFT and CWT techniques, the measured signals were analyzed to detect any variations in frequency and amplitude as well as the presence of nonlinearity during the cutting process. Finally, these results were analyzed to identify any relationship between these phenomena and the tool wear. From the frequency and time-frequency analyzes, the following conclusions were made:

1) In the case of a healthy tool, harmonic and non-harmonic frequencies are present in the nominal values. In the case of a worn tool, these harmonic components either varied from the nominal values or were absent. Additionally, the analysis of the vibration signal shows the presence of new frequencies as the tool wear increases.
2) The analysis of the force amplitudes using FFT does not provide any conclusive evidence to consider it as an indicator of tool wear.
3) Similarly, the analysis on the effect that tool wear has on the nonlinearity levels using CWT does not provide any conclusive evidence to relate these phenomena.

These results are useful for predicting tool breakage in advance. It is also worth noting that the variation in the non-harmonic frequencies is evident from the analysis of the cutting force signal. Further analysis using the vibration signals shows the presence of new frequency components due to tool wear. This implies that the combination of these two process parameters provides more reliable results. Furthermore, the inclusion of the vibration measurement increases the measurement bandwidth. Further studies are expected to include the analysis of measurements at high frequencies ($5,000$Hz to $15,000$Hz).

REFERENCES

[1] R. King, *Handbook of High-Speed Machining Technology*. New York, NY, USA: Springer, 2013.

[2] M. Câmara, J. C. Rubio, A. Abrão, and J. Davim, "State of the art on micromilling of materials, A review," *J. Mater. Sci. Technol.*, vol. 28, no. 8, pp. 673–685, 2012.

[3] M. Malekian, S. S. Park, and M. B. G. Jun, "Tool wear monitoring of micro-milling operations," *J. Mater. Process. Technol.*, vol. 209, no. 10, pp. 4903–4914, 2009.

[4] D. E. D. Snr, "Sensor signals for tool-wear monitoring in metal cutting operations—A review of methods," *Int. J. Mach. Tools Manuf.*, vol. 40, no. 8, pp. 1073–1098, 2000.

[5] C. H. Lauro, L. Brandão, D. Baldo, R. A. Reis, and J. P. Davim, "Monitoring and processing signal applied in machining processes—A review," *Measurement*, vol. 58, pp. 73–86, Dec. 2014.

[6] G. Wang, Y. Yang, and Z. Li, "Force sensor based tool condition monitoring using a heterogeneous ensemble learning model," *Sensors*, vol. 14, no. 11, pp. 21588–21602, 2014.

[7] S. Kurada and C. Bradley, "A review of machine vision sensors for tool condition monitoring," *Comput. Ind.*, vol. 34, no. 1, pp. 55–72, 1997.

[8] D. E. Dimla, Jr., P. M. Lister, and N. J. Leighton, "Neural network solutions to the tool condition monitoring problem in metal cutting—A critical review of methods," *Int. J. Mach. Tools Manuf.*, vol. 37, no. 9, pp. 1219–1241, 1997.

[9] X. Li, "A brief review: Acoustic emission method for tool wear monitoring during turning," *Int. J. Mach. Tools Manuf.*, vol. 42, no. 2, pp. 157–165, 2002.

[10] E. Jantunen, "A summary of methods applied to tool condition monitoring in drilling," *Int. J. Mach. Tools Manuf.*, vol. 42, no. 9, pp. 997–1010, 2002.

[11] B. Sick, "On-line and indirect tool wear monitoring in turning with artificial neural networks: A review of more than a decade of research," *Mech. Syst. Signal Process.*, vol. 16, no. 4, pp. 487–546, 2002.

[12] A. G. Rehorn, J. Jiang, and P. E. Orban, "State-of-the-art methods and results in tool condition monitoring: A review," *Int. J. Adv. Manuf. Technol.*, vol. 26, nos. 7–8, pp. 693–710, 2005.

[13] K. Zhu, Y. S. Wong, and G. S. Hong, "Wavelet analysis of sensor signals for tool condition monitoring: A review and some new results," *Int. J. Mach. Tools Manuf.*, vol. 49, nos. 7–8, pp. 537–553, 2009.

[14] J. V. Abellan-Nebot and F. R. Subirón, "A review of machining monitoring systems based on artificial intelligence process models," *Int. J. Adv. Manuf. Technol.*, vol. 47, nos. 1–4, pp. 237–257, 2010.

[15] R. Teti, K. Jemielniak, G. O'Donnell, and D. Dornfeld, "Advanced monitoring of machining operations," *CIRP Ann.*, vol. 59, no. 2, pp. 717–739, 2010.

[16] S. Dutta, S. K. Pal, S. Mukhopadhyay, and R. Sen, "Application of digital image processing in tool condition monitoring: A review," *CIRP J. Manuf. Sci. Technol.*, vol. 6, no. 3, pp. 212–232, 2013.

[17] M. S. H. Bhuiyan and I. A. Choudhury, "13.22—Review of sensor applications in tool condition monitoring in machining," *Comprehensive Mater. Process.*, vol. 13, pp. 539–569, May 2014.

[18] J.-H. Zhou, C. K. Pang, Z.-W. Zhong, and F. L. Lewis, "Tool wear monitoring using acoustic emissions by dominant-feature identification," *IEEE Trans. Instrum. Meas.*, vol. 60, no. 2, pp. 547–559, Feb. 2011.

[19] C. Aliustaoglu, H. M. Ertunc, and H. Ocak, "Tool wear condition monitoring using a sensor fusion model based on fuzzy inference system," *Mech. Syst. Signal Process.*, vol. 23, no. 2, pp. 539–546, 2009.

[20] Q. Liang, D. Zhang, W. Wu, and K. Zou, "Methods and research for multi-component cutting force sensing devices and approaches in machining," *Sensors*, vol. 16, no. 11, p. 1926, 2016.

[21] N. Fang, P. S. Pai, and S. Mosquea, "Effect of tool edge wear on the cutting forces and vibrations in high-speed finish machining of Inconel 718: An experimental study and wavelet transform analysis," *Int. J. Adv. Manuf. Technol.*, vol. 52, nos. 1–4, pp. 65–77, 2011.

[22] R. E. Haber and J. E. Jiménez, C. R. Peres, and J. R. Alique, "An investigation of tool-wear monitoring in a high-speed machining process," *Sens. Actuators A, Phys.*, vol. 116, no. 3, pp. 539–545, 2004.
[23] T. I. Liu and S. M. Wu, "On-line detection of drill wear," *J. Eng. Ind.*, vol. 112, no. 3, pp. 299–302, 1990.
[24] I. Abu-Mahfouz and A. Banerjee, "Drill wear feature identification under varying cutting conditions using vibration and cutting force signals and data mining techniques," *Proc. Comput. Sci.*, vol. 36, pp. 556–563, Jan. 2014.
[25] B. S. Prasad and M. P. Babu, "Correlation between vibration amplitude and tool wear in turning: Numerical and experimental analysis," *Eng. Sci. Technol., Int. J.*, vol. 20, no. 1, pp. 197–211, 2016.
[26] D. Dimla, Sr., and P. M. Lister, "On-line metal cutting tool condition monitoring.: I: Force and vibration analyses," *Int. J. Mach. Tools Manuf.*, vol. 40, no. 5, pp. 739–768, 2000.
[27] J. Chae and S. S. Park, "High frequency bandwidth measurements of micro cutting forces," *Int. J. Mach. Tools Manuf.*, vol. 47, no. 9, pp. 1433–1441, 2007.
[28] J. Downey, S. Bombiński, M. Nejman, and K. Jemielniak, "Automatic multiple sensor data acquisition system in a real-time production environment," *Proc. CIRP*, vol. 33, pp. 215–220, Jan. 2015.
[29] J. C. Jauregui-correa and O. M. G. Brambila, *Mechanical Vibrations of Discontinuous Systems*. Commack, NY, USA: Nova, 2009.
[30] S.-J. Huang and C.-T. Hsieh, "High-impedance fault detection utilizing a Morlet wavelet transform approach," *IEEE Trans. Power Del.*, vol. 14, no. 4, pp. 1401–1410, Oct. 1999.

JUAN C. JÁUREGUI (SM'10) received the master's degree from the Faculty of Engineering, National Autonomous University of Mexico, Mexico City, Mexico and the Ph.D. degree from the University of Wisconsin–Milwaukee, Milwaukee, WI, USA. He has published more than 50 articles in national and international journals and conferences, as well as the book *Mechanical Vibrations of Discontinuous Systems* (Nova Publishers). His research interests include machine design, structural analysis, and mechanical vibrations. He is a member of the American Society of Mechanical Engineers, the Mexican Society of Mechanical Engineering, IFToMM, and the National System of Researchers in Mexico.

JUVENAL R. RESÉNDIZ (SM'13) received the Ph.D. degree from the Autonomous University of Queretaro, Queretaro, Mexico, in 2010. He was with West Virginia University as a Visiting Professor in 2012. Since 2008, he has been a Professor with the Autonomous University of Queretaro, where he is currently the Chair of the Engineering Automation Program and Master in Automation Program and the Director of Technologic Link. He has worked on industrial and academic automation projects for 15 years. He received several awards for his contributions in developing education technology. He is a member of the Mexican Academy of Sciences and the National Research Academy in Mexico. He is the IEEE Querétaro Section past President.

SURESH THENOZHI (M'17) received the Ph.D. degree in automatic control from the Departamento de Control Automático, Centro de Investigación y de Estudios Avanzados del Instituto Politécnico Nacional, México City, México, in 2014. From 2014 to 2016, he was a Post-Doctoral Researcher with the Faculty of Engineering, Universidad Nacional Autónoma de México, México City. Since 2016, he has been a Research Associate and a Lecturer with the Faculty of Engineering, Universidad Autónoma de Querétaro, Querétaro, México. His current research focuses on intelligent control, structural vibration control, nonlinear vibrations, and contraction analysis. He is a member of the National System of Researchers in Mexico.

TIBOR SZALAY received the Ph.D. degree from the Budapest University of Technology and Economics (BME). He joined BME as an Assistant Professor in 1991, where he is currently an Associate Professor and the Head of the Department of Manufacturing Sciences and Technology. His current research field is focused on manufacturing technology, process measurement, cutting processes, ultra-precision machining, robotics, and assembly automatization. He is a member of the Scientific Society of Mechanical Engineering. He received several fellowships and awards including the Gillemot Prize for the Hungarian Mechanical Engineers and the Knight of Cross from the Order of Merit of the Hungarian Republic.

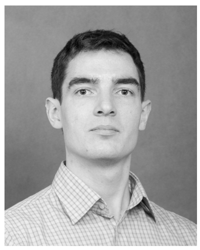

ÁDÁM JACSÓ received the master's degree from the Faculty of Mechanical Engineering, Department of Manufacturing Sciences and Engineering, Budapest University of Technology and Economics, in 2014, where he is currently working towards the Ph.D. degree. The subject of his Ph.D. theme is "Development and Optimization of Pocket Machining Technologies." In addition, he is also interested in micro cutting technology. His main research interest is the planning of modern toolpaths for pocket milling and rough milling operations.

MÁRTON TAKÁCS received the Degree in mechanical engineering and the Ph.D. degree in mechanical engineering sciences from the Budapest University of Technology and Economics (BME) in 1998 and 2007, respectively. He started his research work with the Bay Zoltán Institute for Materials Science and Technology. He is currently an Associate Professor with the Department of Manufacturing Sciences and Technology, BME. He has authored and co-authored more than 70 journal articles and conference papers. His current research field is focusing on experimental and theoretical investigation of machining processes under special circumstances such as micro milling and hard cutting.